A Diguanylate Cyclase Acts as a Cell Division Inhibitor in a Two-Step Response to Reductive and Envelope Stresses

Hyo Kyung Kim, Rasika M. Harshey

Department of Molecular Biosciences and Institute of Cellular and Molecular Biology, University of Texas at Austin, Austin, Texas, USA

ABSTRACT Cell division arrest is a universal checkpoint in response to environmental assaults that generate cellular stress. In bacteria, the cyclic di-GMP (c-di-GMP) signaling network is one of several signal transduction systems that regulate key processes in response to extra-/intracellular stimuli. Here, we find that the diguanylate cyclase YfiN acts as a bifunctional protein that produces c-di-GMP in response to reductive stress and then dynamically relocates to the division site to arrest cell division in response to envelope stress in *Escherichia coli*. YfiN localizes to the Z ring by interacting with early division proteins and stalls cell division by preventing the initiation of septal peptidoglycan synthesis. These studies reveal a new role for a diguanylate cyclase in responding to environmental change, as well as a novel mechanism for arresting cell division.

IMPORTANCE While the major role of c-di-GMP signaling is to control the decision to move freely or settle in a biofilm, recent studies show a broader range of output functions for c-di-GMP signaling. This work reports an unexpected second role for YfiN, a conserved diguanylate cyclase in Gram-negative bacteria, known to contribute to persistence in the host. We find that YfiN acts as a cell division inhibitor in response to envelope stress. Unlike known cell division inhibitors, the interaction of YfiN with cell division proteins retains the Z ring at the midcell but prevents septal invagination. The new function of YfiN not only emphasizes the versatility of c-di-GMP signaling but describes a novel mechanism for a cell division checkpoint.

Bacteria sense and respond to environmental signals through a variety of signaling pathways (1–3). Signaling through the second messenger cyclic di-GMP (c-di-GMP) is ubiquitous in bacteria, where its major role is to control the transition between motile and sessile lifestyles (1, 4). However, recent studies have shown that c-di-GMP also regulates other processes, including cell cycle progression, RNA metabolism, resistance to antimicrobial agents, virulence, and pathogenesis (5–9). Here, we report a new role for c-di-GMP signaling in *Escherichia coli*, where it inhibits cell division in response to envelope stress.

Cellular c-di-GMP levels are set by enzymes that synthesize and degrade this molecule in response to a variety of external and internal signals, both physical and metabolic. Diguanylate cyclases (DGCs), identifiable by a signature GGDEF active-site motif, produce c-di-GMP from GTP, while phosphodiesterases (PDEs), identifiable by an EAL (or HD-GYP) active-site motif, degrade c-di-GMP into pGpG (10). Most DGCs and PDEs harbor various N-terminal sensory input domains, which allow environmental and cellular signals to be integrated into the c-di-GMP signaling network. Although several environmental stimuli regulating DGCs and PDEs have been identified (11–13), the majority of input signals that orchestrate the c-di-GMP signaling network remain to be discovered, especially given the multiplicity of GGDEF/EAL domain proteins in single bacterial species (1).

The DGC YfiN, also called DgcN (14) or TpbB (15), is an inner membrane (IM) protein with a Per-Arnt-Sim (PAS)-like domain in the periplasm and histidine kinase, adenylate cyclase, methyl-accepting protein, and phosphatase (HAMP) and GGDEF domains in the cytoplasm. YfiN has been identified as a key contributor to intracellular c-di-GMP levels in various bacteria, and all of the YfiN-mediated cellular processes described to date are in keeping with the major role of c-di-GMP in inhibiting motility and promoting the biofilm state (15–18). In *Pseudomonas aeruginosa*, where the function of YfiN has been best studied (16, 19), YfiN was found to be regulated by YfiR and YfiB, which are encoded within the same operon (Fig. 1A). The periplasmic protein YfiR is proposed to inhibit YfiN, with the inhibition relieved by reducing conditions that misfold YfiR (19) or by the lipoprotein YfiB that sequesters YfiR to the outer membrane (OM) (Fig. 1B) (16). The *yfi* operon is widespread in Gram-negative bacteria but does not always include *yfiB* (19). For example, *yfiB* is absent in *Salmonella enterica* but present in *E. coli* and *P. aeruginosa* (Fig. 1A). Consistent with the proposal in *P. aeruginosa*, derepression of YfiN caused by disruption of the inhibitor YfiR enhances biofilm formation by activating cellulose production in *E. coli* (18, 20). In *Salmonella*, YfiN was reported to contribute to cellular c-di-GMP levels and inhibit motility through the c-di-GMP receptor YcgR (17). The Yfi system has been suggested to play an important role in the host colonization and persistence of *P. aeruginosa*, as well as a uropathogenic *E. coli* strain (16, 19, 20). We report here a novel second function for YfiN as an inhibitor of cell division in *E. coli* and *Salmonella*, a function promoted by the interaction of YfiN with components of the division machinery.

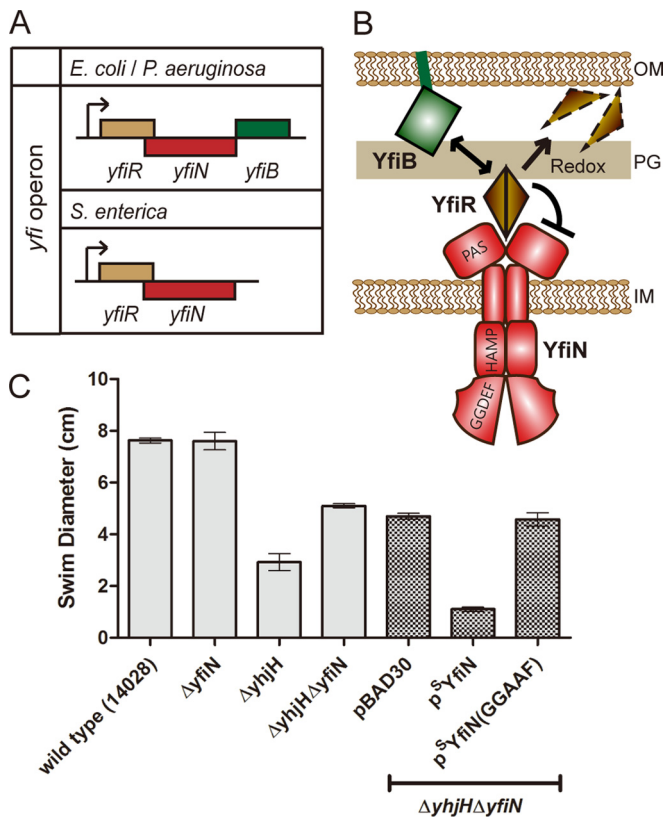Bacterial cell division is orchestrated by the divisome, a dy-

FIG 1 The c-di-GMP-synthetic enzyme YfiN contributes to intracellular c-di-GMP levels in *Salmonella*. (A) *yfi* operon organization in various bacteria. (B) Function of the Yfi system and YfiN domain organization as deduced from studies in *P. aeruginosa* (16, 19). (C) Swimming motility of *S. enterica* wild type (strain 14028) and indicated mutant derivative strains, some carrying an empty vector (pBAD30) or a vector expressing either ^{S}YfiN or its active-site mutant ^{S}YfiN (GGAAF). Overnight cultures of each strain were inoculated at the center of 0.3% agar swim plates supplemented with 0.2% arabinose and incubated at 37°C for 8 h. Error bars indicate standard deviations of the results from four experimental repeats.

namic multiprotein assembly that constricts cell envelope layers at the midcell, timed with completion of DNA replication (21–24). Cell division proteins assemble into the divisome broadly in two steps (23, 24). In an early step, well before the onset of cell constriction and while the cell is still elongating, the tubulinlike protein FtsZ forms a ring at the midcell, which is anchored to the membrane by two proteins, FtsA and ZipA (22, 23). Once assembled, this Z ring recruits downstream components to form a constriction-competent complex, which coordinates septum synthesis and invagination (cytokinesis) (23, 24). While FtsA and ZipA play redundant roles in anchoring the Z ring to the membrane, they are both essential for cytokinesis (22, 23, 25). FtsZ assembly is the major target of cell division checkpoints sensing various stresses, including DNA damage, defective cell wall synthesis, and nutrient starvation (26–29). Here, we show that in both *E. coli* and *Salmonella*, YfiN localizes to the midcell in a Z ring-dependent manner and halts cell division without disassembling the Z ring but, rather, by blocking its further progress toward cytokinesis. In *E. coli*, the midcell localization of YfiN, which requires FtsZ and ZipA, is stimulated by multiple conditions that cause cell envelope stress. Our data suggest that, while the primary

role of the DGC YfiN is to promote biofilm formation under reducing conditions, it has a second role in inhibiting cell division in response to envelope stress.

RESULTS

YfiN contributes to intracellular c-di-GMP levels in *Salmonella* as measured by motility inhibition. The initial impetus for this study was that, with the exception of the PDE YhjH, which was identified as a gatekeeper for maintaining low c-di-GMP levels in the cell and enabling motility (30, 31, 75), it was not known whether any of the other 18 GGDEF/EAL domain proteins in *Salmonella* were involved with motility regulation. Because YhjH would mask the contribution of these 18 proteins to cellular c-di-GMP levels, mutants with mutations in these genes were constructed in a Δ*yhjH* mutant, as well in a wild-type *Salmonella* background and examined for motility in a soft agar plate assay; the data are summarized in Fig. S1 in the supplemental material. Similar data were also recently published independently (17). Of the 18 proteins examined, four were seen to affect motility (see Fig. S1B). Of these, YfiN was observed to contribute most significantly (compare the results for the Δ*yhjH* mutant with those for the Δ*yhjH* Δ*yfiN* mutant in Fig. 1C; see also Fig. S1B). Overexpression of YfiN from an inducible plasmid (p^{S}YfiN) resulted in impaired motility, while an active-site mutant of YfiN (GGDEF→ GGAAF) failed to inhibit motility (Fig. 1C), results consistent with YfiN being a DGC.

Since the experiments described below study YfiN from three different bacteria, *E. coli*, *S. enterica*, and *P. aeruginosa*, we will henceforth use the superscripts E, S, and P, respectively, to indicate the bacterial source of YfiN or other proteins, as necessary. We will also use the subscripts green fluorescent protein (GFP), yellow fluorescent protein (YFP), and cyan fluorescent protein (CFP) for fluorescent fusion proteins, placed before or after the protein to indicate N- or C-terminal locations, respectively.

YfiN accumulates at the midcell in a Z ring-dependent manner and negatively regulates cell division in *Salmonella*. Several GGDEF/EAL proteins have been reported to have a distinct subcellular localization or to exist in a complex with their downstream targets (7, 11, 32–34), prompting us to examine the localization of YfiN. A fusion of GFP to *Salmonella* YfiN (^{S}YfiN$_{GFP}$) was expressed from an inducible plasmid and confirmed to be functional (see Fig. S2A in the supplemental material). In a Δ*yfiN* background, ^{S}YfiN$_{GFP}$ showed as a fluorescent band at the midcell (Fig. 2A), suggesting an association with the cell division machinery. Some of the cells displayed spiral-like structures (Fig. 2A, right), implying that YfiN may associate with the Z ring, whose intermediate structures in various bacteria appear in a spiral/helical configuration at the midcell (35–37). The cytoskeleton protein MreB has also been proposed to polymerize into helical structures in the cell (38), but ^{S}YfiN$_{GFP}$ maintained its structures in the presence of A22, an inhibitor of MreB polymerization (see Fig. S3A). Interestingly, when ^{S}YfiN$_{GFP}$ was at the midcell, no visible cell constriction could be observed (Fig. 2A), whereas in cells with a constriction, ^{S}YfiN$_{GFP}$ was at the quarter positions, which are future division sites (Fig. 2A, arrowheads). These observations indicate that YfiN is likely recruited to the midcell by early division proteins, such as FtsZ, FtsA, and ZipA, prior to constriction.

To detect colocalization of ^{S}YfiN with FtsZ, we used FtsA, the essential division protein that anchors FtsZ to the membrane (22),
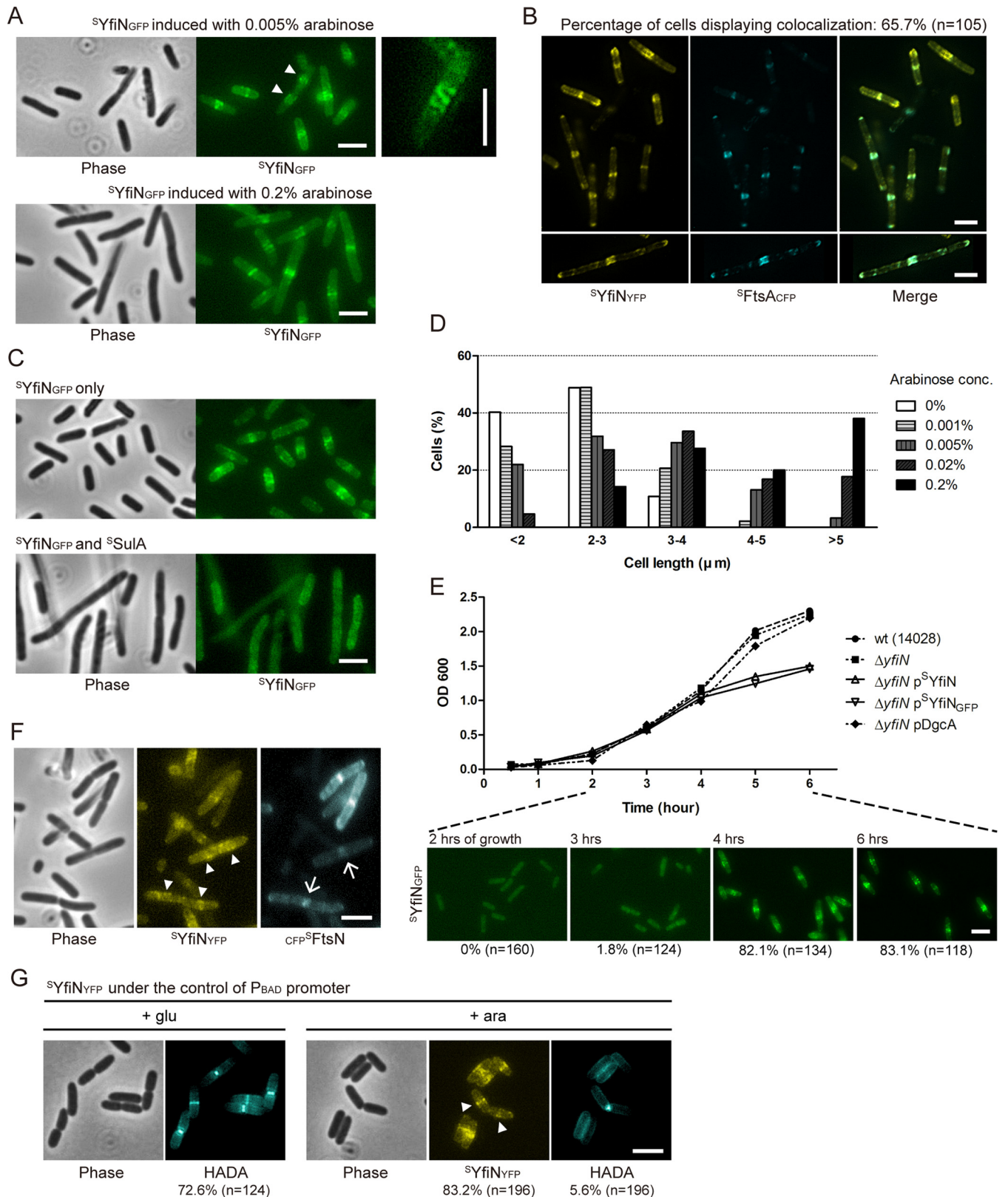
FIG 2 YfiN localizes to the division site, where it inhibits cell division in *Salmonella*. (A) YfiN localization at the midcell. Phase-contrast and fluorescence images of ^{S}YfiN$_{GFP}$ expressed from pBAD30 with different concentrations of inducer arabinose (0.005 and 0.2%) in a *Salmonella* Δ*yfiN* background. Cells with no visible constriction have a fluorescent YfiN band at the midcell, while cells with a constriction show YfiN at the quarter sites (arrowheads). The right panel zooms in on a representative cell showing a spiral structure of ^{S}YfiN$_{GFP}$ at the midcell. Unless otherwise noted, all strains in this study were grown with 0.005% arabinose at 30°C for 4 h before imaging. Scale bars, 3 μm in all images in this study. (B) Colocalization of YfiN and FtsA. ^{S}YfiN$_{YFP}$ and ^{S}FtsA$_{CFP}$ were coexpressed from pBAD

(Continued)

as a proxy, because cells expressing FtsZ fluorescent fusions grew poorly. In cells coexpressing ^{S}YfiN$_{YFP}$ and ^{S}FtsA$_{CFP}$, the two proteins colocalized within rings at the midcell in a majority of the cells (Fig. 2B), as well as within spiral structures along the length of the cell (Fig. 2B, bottom). When the Z ring was disassembled by the expression of the SOS cell division inhibitor SulA (39), ^{S}YfiN$_{GFP}$ failed to localize to the midcell (Fig. 2C). These results suggest that the recruitment of YfiN to the division site is dependent on the assembly of the Z ring.

The accumulation of ^{S}YfiN at the division site was accompanied by cell lengthening in an inducer (arabinose) concentration-dependent manner (Fig. 2A): at 0.2% inducer concentration, cells were approximately twice as long as without inducer (Fig. 2D), indicating that cell division is blocked by YfiN. In addition, cells expressing either ^{S}YfiN or ^{S}YfiN$_{GFP}$ showed a growth defect concomitant with the midcell accumulation of ^{S}YfiN$_{GFP}$ (Fig. 2E). No cell lengthening or growth defect was observed in cells overexpressing a constitutively active DGC, DgcA, from *Caulobacter crescentus* (Fig. 2E) (40), whose activity was confirmed in motility assays (see Fig. S2B in the supplemental material), indicating that the cell division defect caused by YfiN is not merely a consequence of elevated c-di-GMP levels.

The absence of a visible midcell invagination and only a moderate cell lengthening in cells expressing ^{S}YfiN suggests that YfiN inhibits Z ring constriction, as well as septal peptidoglycan (PG) synthesis. Constriction begins after the last essential division protein, FtsN, is recruited to the midcell; the arrival of FtsN has been suggested to activate septal PG synthesis (41, 42). To determine whether YfiN prevents the recruitment of FtsN, we examined the localization of $_{CFP}$^{S}FtsN in cells expressing ^{S}YfiN$_{YFP}$. The majority of cells (79.5%; $n = 239$) expressing both proteins showed the presence of either one or the other protein, but not both, at the midcell (Fig. 2F). While no cell showed colocalization of ^{S}YfiN$_{YFP}$ and $_{CFP}$^{S}FtsN at the midcell, some cells that showed a visible septal invagination (10.4%) exhibited distinct localization of the two fluorescent proteins, with ^{S}YfiN$_{YFP}$ at the quarter positions (Fig. 2F, arrowheads) and $_{CFP}$^{S}FtsN at the constricting septum (arrows).

To examine the effects of YfiN on PG synthesis, we made use of a fluorescent D-amino acid that labels sites of nascent PG synthesis through incorporation into the cell wall (43). In the majority of cells in which the expression of ^{S}YfiN$_{YFP}$ was repressed by glucose, the blue-fluorescent D-amino acid HADA was found incorporated as a band at the midcell, regardless of whether a cell constriction was visible (Fig. 2G). In contrast, when the expression of ^{S}YfiN$_{YFP}$ was induced by arabinose, the number of cells showing HADA at the midcell decreased from 72.6% to 5.6% (Fig. 2G, compare + glu

to + ara), which indicates that YfiN inhibits septal PG synthesis. In the 5.6% of cells that showed HADA at the constriction site, ^{S}YfiN$_{YFP}$ was exclusively at the quarter sites (Fig. 2G, arrowheads). The stalled septal PG synthesis and the distinct localization patterns of YfiN and FtsN raise the possibility that YfiN accumulation prevents the Z ring from maturing into a constriction-competent division complex, possibly by inhibiting the recruitment of late division proteins.

YfiN is recruited to the division site in response to cell envelope stress in *E. coli*. To determine whether YfiN has the same cell division arrest function in the closely related bacterium *E. coli*, a GFP fusion of *E. coli* YfiN (^{E}YfiN$_{GFP}$) was constructed and confirmed to be functional (see Fig. S2B in the supplemental material). Analysis of intracellular c-di-GMP levels in cells expressing ^{E}YfiN$_{GFP}$ was consistent with the designation of ^{E}YfiN as a DGC (see Materials and Methods). When expressed in an *E. coli* $\Delta yfiN$ background, ^{E}YfiN$_{GFP}$ localized to the midcell, concomitant with a growth defect (Fig. 3A), similar to the experiment whose results are shown in Fig. 2E. A membrane-dispersed localization of ^{E}YfiN$_{GFP}$ was clearly evident until the mid-log phase (after 4 h of growth), and one or more hours of further growth was required for ^{E}YfiN$_{GFP}$ to relocate to the midcell (Fig. 3A).

The relocation of ^{E}YfiN$_{GFP}$ to the midcell near the stationary phase of growth suggested that the midcell localization might be a response to depletion of nutrients, changes in pH, or some other stressful condition. Previous studies in *P. aeruginosa* and *E. coli* have shown that misfolding of the periplasmic inhibitor YfiR caused by reducing environments leads to activation of YfiN, identifying reductive stress as one of the input signals of the Yfi system (18, 19). Additionally, in *P. aeruginosa*, the Yfi system was proposed to contribute to biofilm formation under cell envelope stress conditions like osmotic upshift and exposure to the detergent sodium dodecyl sulfate (SDS) (19). To identify input stimuli that promote the observed ^{E}YfiN relocation to the midcell, we tested conditions suggested to activate the Yfi system in previous studies and a variety of other stressors as well, including nutrient starvation and acid stress. Cells producing ^{E}YfiN$_{GFP}$ were exposed to a stress condition after 4 h of growth, when ^{E}YfiN$_{GFP}$ was still dispersed throughout the membrane (Fig. 3A). Of the many stressors tested, only the following conditions were observed to trigger ^{E}YfiN$_{GFP}$ relocation within 30 min of exposure at room temperature: osmotic upshift with either NaCl (250 mM) or sucrose (10%) and treatment with the envelope-targeting antibiotic polymyxin B (PMB; 2.5 μg/ml) (Fig. 3B). These treatments stimulated ^{E}YfiN relocation in a concentration-dependent manner (see Fig. S4A and B in the supplemental material); osmotic downshift

---

Figure Legend Continued

plasmids in $\Delta yfiN$ cells. The bottom panels show a representative cell displaying colocalization of ^{S}YfiN$_{YFP}$ and ^{S}FtsA$_{CFP}$ in a spiral structure along the membrane. (C) Localization of YfiN in the absence and presence of SulA. After 3 h of growth, the expression of ^{S}YfiN$_{GFP}$ and ^{S}SulA from pBAD plasmids was induced in a $\Delta yfiN$ strain, and cells were grown for one further hour before imaging. (D) Histogram of cell length distribution of $\Delta yfiN$ cells expressing ^{S}YfiN with different concentrations of the inducer arabinose. Cell length was measured manually as the distance between two poles, and the distribution is shown as percentages of cells in the indicated ranges. The cell numbers in different concentrations of arabinose were as follows: 0%, $n = 154$; 0.001%, $n = 192$; 0.005%, $n = 191$; 0.02%, $n = 197$; and 0.2%, $n = 210$. (E) Growth curves of the wild type (strain 14028) and its $\Delta yfiN$ and $\Delta yfiN$ derivatives expressing ^{S}YfiN, ^{S}YfiN$_{GFP}$, or DgcA from pBAD30. The inducer arabinose (0.005%) was added at time zero in this experiment, and the localization of ^{S}YfiN$_{GFP}$ at selected time points is shown below. The percentages of cells showing ^{S}YfiN$_{GFP}$ at the midcell and the total number of cells counted are shown below the images. (F) Localization of YfiN and FtsN. ^{S}YfiN$_{YFP}$ and $_{CFP}$^{S}FtsN were coexpressed from pBAD plasmids in $\Delta yfiN$ cells. Arrowheads denote localization of ^{S}YfiN to the quarter positions, and arrows indicate ^{S}FtsN foci localizing at midcell constriction sites. (G) Nascent peptidoglycan synthesis in cells expressing YfiN. $\Delta yfiN$ cells expressing ^{S}YfiN$_{YFP}$ from pBAD33 were grown with either glucose or arabinose and labeled with the blue-fluorescent D-amino acid HADA for 1 min. The percentages of cells displaying HADA or ^{S}YfiN$_{YFP}$ at the midcell and the total number of cells counted are shown below the images.
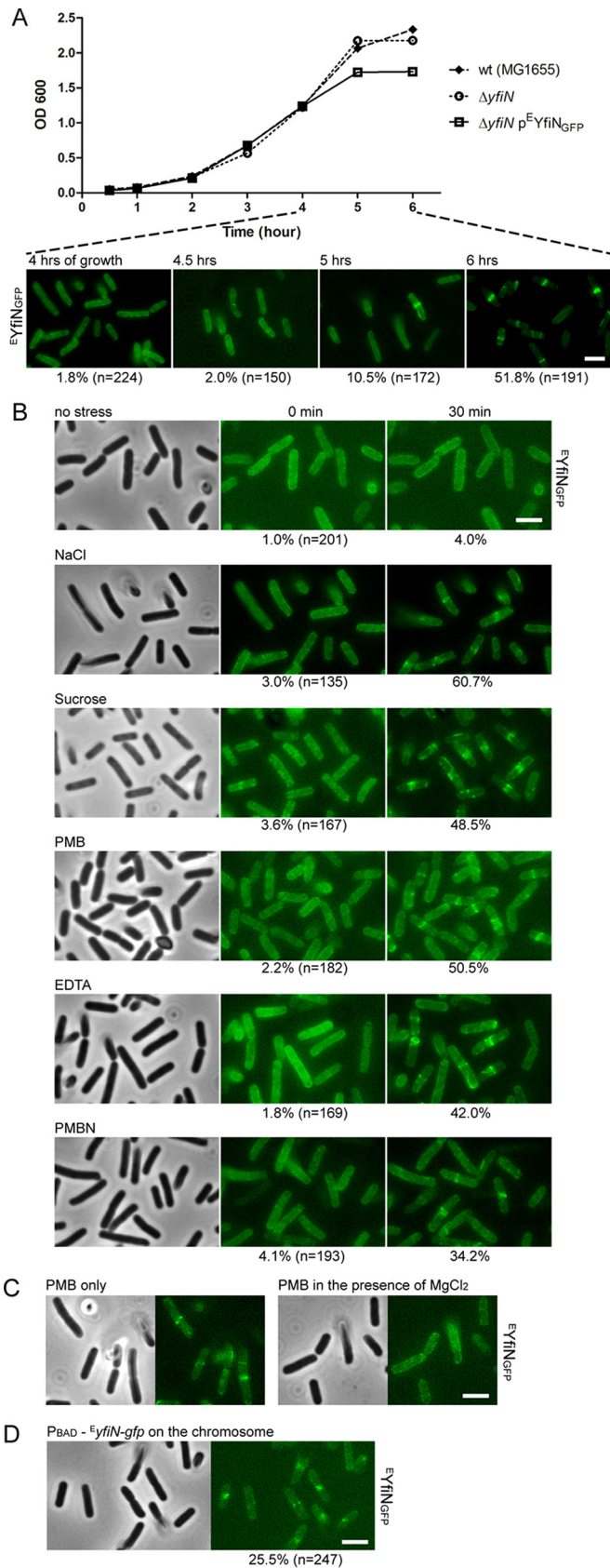
FIG 3 YfiN relocates to the midcell in response to envelope stress in *E. coli*. (A) Growth curves of *E. coli* wild-type (strain MG1655) cells, Δ*yfiN* cells, or

(Continued)

had no impact. No new protein synthesis was required for this response (see Fig. S5).

PMB, a polycationic molecule, is thought to increase cell permeability in Gram-negative bacteria by interacting with both the outer membrane (OM) and inner membrane (IM) in a dual mechanism of action (44–46). PMB first binds to the negative charges on lipopolysaccharide (LPS) and removes the divalent cations that stabilize the LPS structure (44, 45). This results in an increase in OM permeability, which allows PMB to penetrate into the IM, causing leakage of cell contents and cell death (44, 45). To determine whether alteration of the OM or the IM stimulates the ^{E}YfiN relocation, we tested two more agents, EDTA and polymyxin B nonapeptide (PMBN). EDTA is a strong divalent cation chelator known to disrupt the OM in the same manner as PMB, but EDTA is not an IM stressor (44, 46). The polymyxin derivative PMBN is less lethal than PMB due to the absence of the fatty acid tail required for the IM disruption, but PMBN still retains the ability to permeabilize the OM (44). Both of the OM-permeabilizing agents, EDTA (10 mM) and PMBN (200 μg/ml), induced midcell localization of ^{E}YfiN$_{GFP}$ (Fig. 3B), indicating that OM disruption is most likely the trigger for ^{E}YfiN relocation. In agreement with the known property of high divalent cation concentrations in blocking the effect of PMB on OM permeabilization (44), the addition of external MgCl$_2$ (10 mM) prevented PMB treatment from triggering ^{E}YfiN$_{GFP}$ relocation (Fig. 3C). Other membrane-targeting agents, including a β-lactam antibiotic, SDS, and lysozyme, failed to relocate ^{E}YfiN$_{GFP}$ (see Fig. S4C in the supplemental material). Taken together, these data suggest that envelope stress caused by osmotic upshift or OM permeabilization by divalent ion extraction is the input signal for ^{E}YfiN to relocate to the division site.

While ^{E}YfiN$_{GFP}$ relocated to the midcell in response to envelope stress, the same conditions had no effect on ^{S}YfiN$_{GFP}$ localization in *Salmonella* (not shown). This observation led us to hypothesize that the lipoprotein YfiB, which is absent in *Salmonella*, might function as a sensor that couples envelope stress to ^{E}YfiN localization (Fig. 1A and B). It is worth noting that YfiB is a structural homolog of Pal, a component of the Tol-Pal complex that plays a crucial role in maintaining OM integrity in Gram-negative bacteria (47, 48). However, in a *yfiB* knockout mutant of *E. coli*, ^{E}YfiN$_{GFP}$ still retained its ability to relocate upon envelope stress (not shown), indicating that YfiB is not involved in the ^{E}YfiN relocation.

Next, we fused GFP to the *yfiN* chromosomal locus in *E. coli* to

Figure Legend Continued

Δ*yfiN* cells expressing ^{E}YfiN$_{GFP}$ from pBAD30 with the inducer arabinose added at time zero. The localization of ^{E}YfiN$_{GFP}$ at selected time points is shown in the images below. (B) ^{E}YfiN relocation to the midcell upon envelope stress. *E. coli* Δ*yfiN* cells expressing ^{E}YfiN$_{GFP}$ were exposed to the indicated stresses. The same microscope fields were photographed before and 30 min after exposure to no stress (LB medium only), osmotic upshift (LB with 250 mM additional NaCl or 10% sucrose), or OM permeabilization (LB with 2.5 μg/ml PMB, 10 mM EDTA, or 200 μg/ml PMBN). For each stressor, the same field of cells was observed to count the fraction of cells showing midcell foci. (C) Effect of added Mg^{2+} on PMB-triggered ^{E}YfiN relocation. *E. coli* Δ*yfiN* cells expressing ^{E}YfiN$_{GFP}$ were exposed to 2.5 μg/ml PMB for 30 min in the absence and presence of 10 mM MgCl$_2$. (D) Localization of ^{E}YfiN$_{GFP}$ expressed from the chromosomal inducible promoter. An *E. coli* *yfiR::kan* mutant strain, in which ^{E}*yfiN-gfp* is carried under the P$_{BAD}$ promoter on the chromosome, was grown with arabinose at 30°C for 4 h and exposed to 250 mM NaCl for 30 min.

observe the localization of endogenously expressed [E]YfiN. However, [E]YfiN$_{GFP}$ expressed under its native promoter failed to display enough fluorescence to be observed regardless of exposure to stress (not shown). When the native promoter was replaced with an inducible promoter (P$_{BAD}$), [E]YfiN$_{GFP}$ expressed from the chromosomal locus was able to show relocation upon the envelope stress (Fig. 3D). These data suggest that a single copy on the chromosome is sufficient to produce [E]YfiN serving as a cell division inhibitor, but it requires activation at the transcriptional level by as-yet-unknown signals.

Localization of [E]YfiN to the division site is dependent on its interaction with FtsZ and ZipA. Having observed that [S]YfiN is associated with the Z ring (Fig. 2B and C), we monitored [E]YfiN$_{GFP}$ localization in temperature-sensitive mutants of *E. coli* cell division proteins in order to validate specific binding targets of [E]YfiN. We used *ftsZ84* (strain WM1125), *ftsA12* (strain WM1115), and *zipA1* (strain PS223) mutant strains that are defective in the assembly/recruitment of the respective protein to the division site at the nonpermissive temperature (42°C). The essential division proteins FtsA and ZipA serve as redundant membrane anchors for the Z ring (22, 25). At the nonpermissive temperature (42°C), lack of Z ring assembly in the *ftsZ84* mutant results in loss of localization of all divisome components (49). The absence of either FtsA or ZipA in the *ftsA12* or *zipA1* mutant at 42°C is not expected to disrupt the Z ring because FtsZ remains at the midcell as long as either one of these proteins is present, but assembly of downstream components that mediate cytokinesis is inhibited in both of these mutants (25, 49).

The *E. coli* mutant cells expressing [E]YfiN$_{GFP}$ were first exposed to PMB for 30 min at room temperature to promote [E]YfiN relocation and then shifted to 30°C or 42°C for another 30 min. At 30°C, [E]YfiN$_{GFP}$ remained in spiral/ring structures at the midcell in a wild-type background and in all three mutants (Fig. 4A). At 42°C, while wild-type cells maintained [E]YfiN$_{GFP}$ at the midcell, both the *ftsZ84* and the *zipA1* mutant lost the localization and showed dispersed clusters of [E]YfiN$_{GFP}$ (Fig. 4A), suggesting that [E]FtsZ and [E]ZipA are essential for [E]YfiN localization. In contrast, [E]YfiN$_{GFP}$ localization was unaffected in the *ftsA12* mutant at 42°C (Fig. 4A), indicating that [E]YfiN$_{GFP}$ localization to the midcell does not require [E]FtsA and, therefore, also does not require cell division components that act downstream from [E]FtsA. NaCl was not used as a stressor in these experiments because the *ftsZ84* mutation can be suppressed by high salt (50). However, similar results were obtained when EDTA was used as a stressor (see Fig. S6 in the supplemental material). In summary, these data show that [E]YfiN localization at the midcell depends on the [E]FtsZ ring and its [E]ZipA tether but not on [E]FtsA or downstream events known to be dependent on [E]FtsA assembly.

To further investigate interactions between [E]YfiN and the cell division proteins, the bacterial adenylate cyclase two-hybrid (BACTH) assay was performed. The BACTH assay has been used successfully for analyzing interactions between membrane proteins, including cell division and cytoskeleton proteins (51, 52). For this assay, FtsZ, FtsA, ZipA, and YfiN from *E. coli* were fused to two fragments of the *Bordetella pertussis* adenylate cyclase, T18 and T25, and their interaction was monitored by measuring the synthesis of β-galactosidase, which is dependent on the adenylate cyclase activity. The results showed self-interaction of [E]YfiN (Fig. 4B), which is expected because dimerization is required for DGCs to exert their enzymatic activity (53). A positive result was
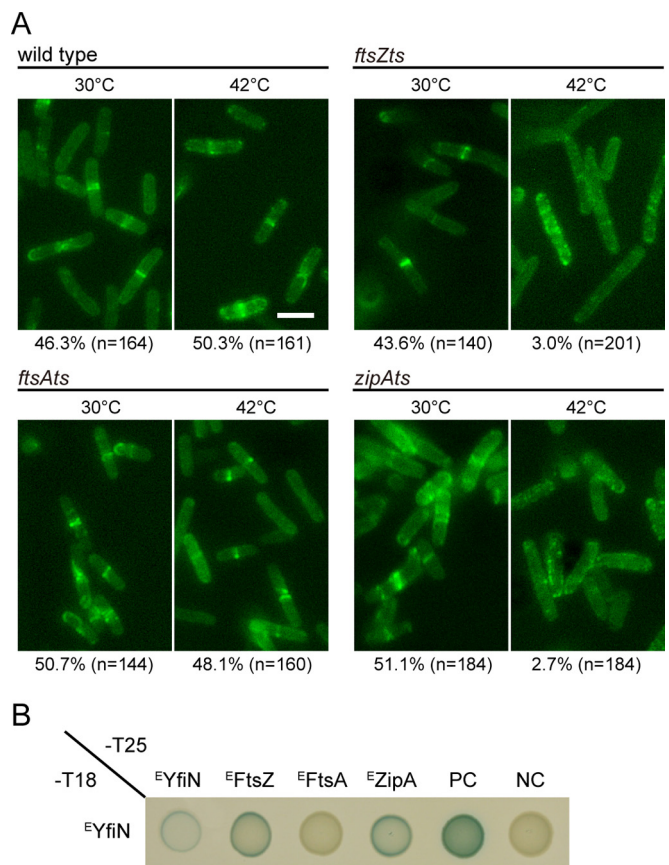

FIG 4 YfiN interacts with FtsZ and ZipA in *E. coli*. (A) Localization of [E]YfiN$_{GFP}$ in wild-type (MG1655) cells and temperature-sensitive (ts) mutants with mutations of cell division proteins in *E. coli*. For each strain, cells producing [E]YfiN$_{GFP}$ were exposed to 2.5 µg/ml PMB for 30 min. Following the exposure, cells were incubated for another 30 min at two different temperatures, 30°C and 42°C, before imaging. (B) Bacterial adenylate cyclase two-hybrid (BACTH) analysis of *E. coli* division proteins against [E]YfiN. Either the T18 or T25 fragment was fused to the C-terminal ends of [E]YfiN and the cell division proteins. PC, positive control (T18-leucine zipper/T25-leucine zipper); NC, negative control (T18/T25 empty vectors).

obtained with [E]YfiN and either [E]FtsZ or [E]ZipA, supporting their interaction (Fig. 4B). No interaction was detected between [E]YfiN and [E]FtsA (Fig. 4B), in agreement with the persistence of [E]YfiN$_{GFP}$ at the midcell in the *ftsA12* mutant at 42°C (Fig. 4A). The cytoskeletal protein [E]MreB, previously shown to colocalize with [E]FtsZ and directly interact with it using the BACTH assay (52), showed interaction with [E]FtsZ but not with [E]YfiN (see Fig. S3B in the supplemental material). Taken together, the data in Fig. 4 and in Fig. S3 in the supplemental material show that [E]YfiN relocation at the midcell is dependent on [E]FtsZ and [E]ZipA but not on [E]FtsA or [E]MreB.

High intracellular c-di-GMP levels are required for midcell localization of YfiN in *E. coli*. Given the unexpected role of the c-di-GMP-synthetic enzyme YfiN in cell division regulation, we wondered whether the DGC activity of YfiN was required for its cell division arrest function or whether this was a separate function of YfiN. We therefore inactivated the DGC active site of [E]YfiN$_{GFP}$ (GGDEF→GGAAF). Like the wild-type protein, the mutant protein was evenly distributed throughout the membrane before exposure to stress but failed to localize to the midcell when
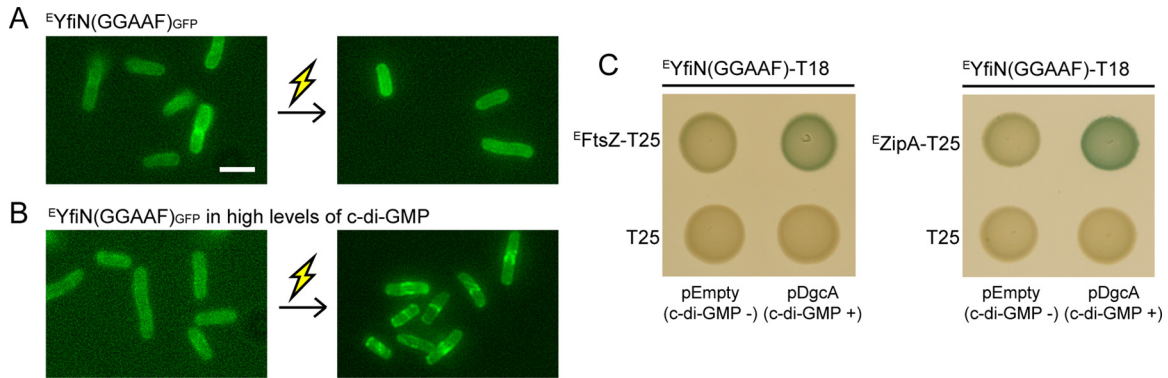
FIG 5 High levels of c-di-GMP provided by a heterologous DGC restore midcell relocation of an active-site mutant of *E. coli* YfiN. (A and B) *E. coli* Δ*yfiN* cells expressing ᴱYfiN(GGAAF)_GFP alone (A) or with the *C. crescentus* DGC DgcA (B) were grown with inducer [arabinose for ᴱYfiN(GGAAF)_GFP and 0.01 mM IPTG for DgcA] at 30°C for 4 h and exposed to 250 mM NaCl. Images were taken before and 30 min after the osmotic upshift. Thunderbolt represents envelope stress. (C) BACTH analysis of c-di-GMP-stimulated interaction between ᴱYfiN(GGAAF) and cell division proteins ᴱFtsZ and ᴱZipA. Along with the T18 and T25 constructs, each strain contains an empty pBAD33 or a plasmid carrying *dgcA*, whose expression was induced with 0.2% arabinose. Overexpression of DgcA alone did not affect the results of BACTH, as shown with control strains in the bottom row.

exposed to osmotic upshift (Fig. 5A), suggesting that relocation of YfiN to the division site is dependent on the DGC activity. To determine whether the requirement for the DGC activity can be bypassed by high levels of c-di-GMP, we provided c-di-GMP artificially by expressing the constitutively active heterologous DGC DgcA (40). Under this condition, the mutant ᴱYfiN was able to relocate to the midcell in response to envelope stress (Fig. 5B). This suggests that high intracellular c-di-GMP levels are required for ᴱYfiN to interact with cell division proteins. To assess the c-di-GMP dependence of YfiN interaction with division proteins, BACTH analysis was performed again. The interaction of the mutant ᴱYfiN with ᴱFtsZ or ᴱZipA was observed to be strengthened in the presence of DgcA (Fig. 5C), consistent with the localization data (Fig. 5B). These results suggest two possible models: (i) c-di-GMP directly binds to ᴱYfiN, which then causes its direct interaction with cell division proteins, and (ii) c-di-GMP indirectly promotes ᴱYfiN interaction with cell division proteins via some other factor that binds c-di-GMP.

Midcell relocation of YfiN in response to envelope stress requires release of its periplasmic inhibitor YfiR by reductive stress in *E. coli*. The periplasmic protein YfiR inhibits the c-di-GMP-synthetic activity of YfiN by interacting with the PAS-like domain of YfiN in the periplasm (16, 18, 20). To assess whether YfiR also counteracts the function of YfiN in cell division, ᴱYfiR was coexpressed with ᴱYfiN_GFP in *E. coli*. In the presence of ᴱYfiR, ᴱYfiN_GFP remained localized throughout the membrane and failed to relocate to the midcell when cells were exposed to envelope stress (compare Fig. 6A and B). These results indicate that ᴱYfiR is a repressor of the cell division arrest function of ᴱYfiN as well.

Previous studies in *P. aeruginosa* and *E. coli* suggested that YfiR is a periplasmic redox sensor that regulates YfiN activity in response to reducing conditions (18, 19). YfiR has two pairs of conserved cysteine residues whose intramolecular disulfide bonds play important roles in dimerization (54). Reducing environments are thought to disrupt the disulfide bonds in YfiR, thus derepressing YfiN (18, 19, 54). To test whether the inhibitory effect of ᴱYfiR on ᴱYfiN relocation can be relieved by reducing conditions, *E. coli* cells coexpressing ᴱYfiN_GFP and ᴱYfiR were

treated with the reducing agent dithiothreitol (DTT). When DTT was added to a final concentration of 10 mM for 1 h prior to envelope stress exposure, ᴱYfiR lost its ability to repress ᴱYfiN relocation (Fig. 6C). Similar results were obtained in the absence of DsbA, a protein responsible for disulfide bond formation in periplasmic proteins (Fig. 6D). The inactivation of the disulfide bonding system (DSB) has been reported to relieve the repression of YfiN by YfiR (18, 19). Under both reducing conditions (Fig. 6C and FigD), ᴱYfiN remained dispersed in the membrane until exposed to envelope stress, which indicates that the release of ᴱYfiR is required but not sufficient for the relocation of ᴱYfiN. These results were also supported by the results in a *yfiR* knockout mutant (Fig. 6E).

Overall, these data identify ᴱYfiN as a sensor that detects two different extracellular signals. A reductive stress signal is required to inactivate the inhibitor ᴱYfiR and turn on the DGC activity of ᴱYfiN, which is essential for responding to envelope stress and relocating YfiN to the midcell (Fig. 5). Thus, ᴱYfiN senses and responds to two sequential signals—reductive and envelope stresses—before arresting cell division.

YfiN upregulation offers protection against polymyxin B in *E. coli*. The dynamic relocation of ᴱYfiN to the division site in response to potentially lethal envelope stressors suggests that this response might provide protection and/or facilitate adaptation under such conditions. To test this, we examined the following several strains for their susceptibility to PMB: wild-type *E. coli* strain MG1655, the Δ*yfiN* mutant, a strain carrying *yfiN-gfp* at its native chromosomal locus, and Δ*yfiR* and Δ*yfiR* mutants with ᴱYfiN_GFP expressed from the chromosomal inducible promoter (also used in the experiment whose results are shown in Fig. 3D). Of these strains, only the one with ectopic expression of ᴱYfiN from the chromosomal inducible promoter showed an approximately 10-fold increase in survival after 30 min of exposure to PMB (2.5 μg/ml) (Fig. 7). While these data do not address whether the division arrest function of ᴱYfiN is the cause of increased cell survival, they implicate ᴱYfiN in participating in bacterial defense mechanisms against envelope stress. There was no difference in survival between the wild type and the Δ*yfiN* strain, indicating that the ᴱ*yfiN* gene under the control of

A ^EYfiN_GFP only
70.2% (n=228)

B ^EYfiN_GFP and ^EYfiR
3.9% (n=232)

C ^EYfiN_GFP and ^EYfiR - pretreated with DTT
63.6% (n=217)

D ^EYfiN_GFP and ^EYfiR in *dsbA::kan*
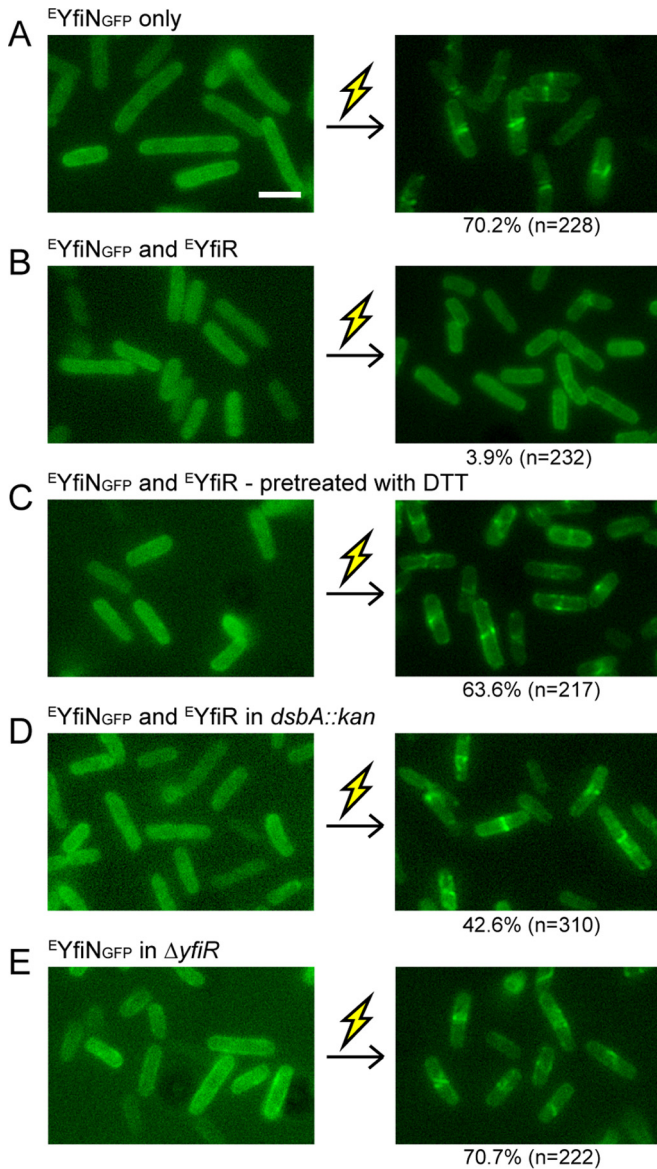42.6% (n=310)

E ^EYfiN_GFP in Δ*yfiR*
70.7% (n=222)

FIG 6 YfiR prevents YfiN relocation to the midcell in *E. coli*. Cells were grown with inducer (arabinose for ^EYfiN_GFP and 0.01 mM IPTG for ^EYfiR) at 30°C for 4 h and exposed to 250 mM NaCl. Images were taken before and 30 min after the osmotic upshift. Thunderbolt represents envelope stress. (A) *E. coli* Δ*yfiN* cells expressing ^EYfiN_GFP only. (B) *E. coli* Δ*yfiN* cells expressing ^EYfiN_GFP and ^EYfiR. (C) *E. coli* Δ*yfiN* cells expressing ^EYfiN_GFP and ^EYfiR. Ten millimoles DTT was added to the culture 1 h prior to osmotic upshift. (D) *E. coli* *dsbA::kan* cells expressing ^EYfiN_GFP and ^EYfiR. (E) *E. coli* Δ*yfiR* cells expressing ^EYfiN_GFP only.

MG1655	- PMB	+ PMB
wt		
Δ*yfiN*		
yfiN::yfiN-gfp		
yfiR::kan		
yfiR::kan P_BAD::*yfiN-gfp*		
wt pDgcA		

FIG 7 Ectopically expressed ^EYfiN enhances cell viability after exposure to polymyxin B. After growth to the mid-log phase (at 30°C for 4 h) with 0.005% arabinose, the indicated strains were incubated with or without 2.5 μg/ml PMB for 30 min at room temperature and plated in 10-fold dilutions (10^{-1} to 10^{-6}) on LB agar plates. In the *yfiR::kan* mutants, the *kan* cassette is inserted in an orientation opposite to the direction of *yfi* operon transcription in order to avoid polar effects on the downstream *yfiN* gene.

tween motile and sedentary bacterial lifestyles, the function of c-di-GMP has steadily expanded to include a remarkably diverse set of cellular processes. In this work, we establish a new and unique role for the diguanylate cyclase YfiN as both an enzyme and an effector that stalls cell division by interacting with early cell division proteins in *E. coli* and *Salmonella*.

YfiN as a sensor for multiple environmental stresses. In both *Salmonella* and *E. coli*, YfiN localizes to the division site and arrests cell division, which is exerted through interaction with cell division proteins (Fig. 2, 3, and 4). In *E. coli*, the trigger for recruitment of YfiN to the midcell is osmotic upshift and membrane permeabilization (Fig. 3B). The OM permeabilizers that stimulate ^EYfiN relocation—PMB, EDTA, and a high concentration of PMBN (Fig. 3B)—have all been reported to induce the release of LPS and leakage of periplasmic proteins by altering LPS-LPS interactions in the OM (44, 56). Hyperosmotic stress also causes periplasmic contents to leak out (44, 57). This common attribute of the agents suggests that periplasmic leakage might be the specific input signal for the ^EYfiN-mediated cell division inhibition. One might then imagine that loss of the periplasmic protein YfiR by periplasmic leakage might be the trigger of ^EYfiN relocation, given the function of YfiR as an inhibitor of YfiN (16, 18). However, this is not the case, because inactivation of ^EYfiR by either reductive stress or genetic mutation was not enough to relocate ^EYfiN to the midcell without envelope stress (Fig. 6C, D, and E). Thus, ^EYfiN is a membrane-associated sensor that responds to two independent environmental cues, reductive and envelope stresses.

While midcell localization of YfiN in *E. coli* is stimulated by osmotic upshift and OM permeabilization, the same conditions did not lead to a change in YfiN localization in *Salmonella* (not shown), suggesting that the signals that cause division arrest by YfiN differ between *E. coli* and *Salmonella*. In both bacteria, YfiN midcell localization was dependent on the growth phase (Fig. 2E and 3A), but the exact stress sensed in the stationary phase is not known. Surprisingly, *P. aeruginosa* YfiN does not localize to the division site either during the stationary phase or with envelope stress exposure in any of the bacterial species tested (see Fig. S7 in the supplemental material). Thus, despite its overall conservation as a c-di-GMP-synthetic enzyme, YfiN appears to have evolved to acquire an additional cell division arrest function in *E. coli* and *Salmonella*, which is activated in response to different environmental signals.

Thus far, DGCs are known to produce c-di-GMP in response

its native promoter needs to be upregulated by unknown signals in order to offer protection. The data also show that the protection against PMB is not simply a consequence of elevated c-di-GMP levels, because overexpression of DgcA did not increase survival (Fig. 7).

DISCUSSION

Since the original discovery of c-di-GMP as an allosteric effector of a bacterial cellulose synthase (55) and the later revelation of its major role as a second messenger that controls the decision be-
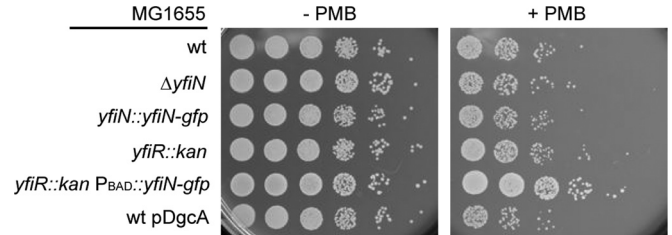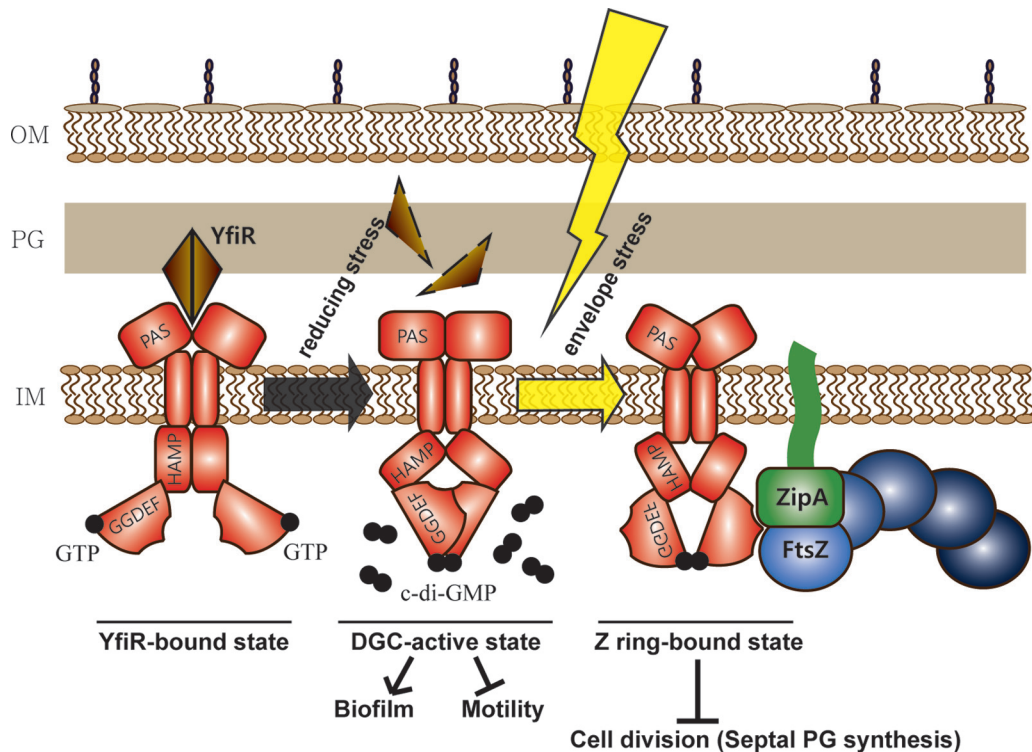
FIG 8 Model for YfiN as a cell division inhibitor. [E]YfiN is a bifunctional protein that responds to two different environmental stresses—reductive and envelope stress. The DGC function is known to be activated when reductive stress inactivates the periplasmic repressor [E]YfiR. The c-di-GMP thus produced inhibits motility and activates biofilm formation. The second function of [E]YfiN as a cell division inhibitor, as revealed in this study, requires an additional envelope stress after the DGC function is activated. The envelope stress-induced conformation of [E]YfiN, which is likely in a c-di-GMP-bound state, exposes binding sites for division proteins FtsZ and ZipA, directing [E]YfiN to the future division site, where it halts division by preventing the initiation of septal peptidoglycan synthesis.

to environmental cues, and c-di-GMP then serves as a second messenger that binds to a protein or an RNA effector and elicits a downstream response. A DGC-inactive [E]YfiN regained the ability to interact with cell division proteins when intracellular c-di-GMP levels were elevated (Fig. 5B and C). This suggests that [E]YfiN in a c-di-GMP-bound state itself might be the effector that interacts with the division proteins. Alternatively, c-di-GMP could bind to some other division protein that in turn promotes the recruitment of [E]YfiN to the division site. However, the latter possibility is less likely because, while the c-di-GMP-binding proteins known to date include many GGDEF domain proteins, they do not include those constituting the divisome machinery (58). Although [E]YfiN does not have a conserved I site (RXXD motif), which is the best characterized c-di-GMP-binding site in GGDEF domain proteins, a recent study reported an example of a DGC that exists in a complex with c-di-GMP even when it has no I site (59). We therefore favor the idea that high levels of c-di-GMP might enhance the interaction of [E]YfiN with division proteins by binding to [E]YfiN and stabilizing the conformational change induced by envelope stress.

Based on these results, we propose a model in which [E]YfiN acts as a bifunctional protein exhibiting both enzymatic and effector activities (Fig. 8). The enzymatic function of [E]YfiN is activated by the release of [E]YfiR under reducing conditions, and the c-di-GMP thus generated impairs motility and enhances biofilm formation (18, 20). The effector function exerted by c-di-GMP-bound [E]YfiN requires an additional envelope stress cue, which likely results in an additional conformation change that exposes binding sites on

[E]YfiN to the division proteins FtsZ and ZipA, leading to cell division arrest.

The idea of bifunctional GGDEF/EAL domain proteins acting as an enzyme and an effector was previously proposed for a couple of PDEs, YciR (also called PdeR) (33) and PdeL (60). Such bifunctionality of a DGC/PDE, now seen with YfiN, would achieve local specificity of c-di-GMP signaling, since the second function is restricted to distinct downstream targets by their specific spatial organization. All of these examples share a requirement for enzymatic activity for their dual action, but YfiN requires an additional input signal, envelope stress, to serve its second function of cell division control. While we accidentally unearthed the distinct responses of YfiN to different stimuli, such multitasking may be common in c-di-GMP signaling, enabling bacteria to respond differentially to multiple environmental challenges.

YfiN as a cell division checkpoint for adaptation to envelope stress. From bacteria to eukaryotes, cell division regulation is used as a checkpoint to ensure survival upon exposure to stress. In bacteria, DNA damage (28) or envelope stress caused by inactivation of the peptidoglycan synthase PBP 3 (29) triggers the SOS response, in which the expression of the cell division inhibitor SulA is activated. While SulA directly inhibits FtsZ polymerization and leads to disassembly of the Z ring (39), YfiN retains the Z ring at the midcell (Fig. 2E and 3A). This feature of YfiN as a cell division inhibitor can also be observed with two DNA damage-induced proteins, SidA and DidA, in *C. crescentus*, a bacterium that does not have a SulA homolog. SidA and DidA arrest cell division by inhibiting late cell division events while retaining the Z

ring (61, 62). Unlike SidA and DidA, however, cells with YfiN at the midcell have no visible constriction site (Fig. 2A), suggesting that YfiN inhibits the initiation of constriction. Although precisely which step in cell division is blocked by YfiN is not yet clear, exclusion of the late division protein FtsN and stalled septal PG synthesis at the future division sites occupied by YfiN raise the possibility that YfiN inhibits the initiation of constriction by using early division proteins as docking sites and preventing the recruitment of late division proteins (Fig. 2F and G). It has been reported that the interplay between FtsN and two early division proteins, FtsA and ZipA, is essential for the activation of constriction (41, 42), which might be affected by YfiN. We also note that some cells expressing YfiN$_{GFP}$ show wide rings at the midcell, which are often slanted or off center (Fig. 4 to 6; see also Fig. S5 to S6 in the supplemental material), reminiscent of FtsZ structures seen under several conditions, including mutations in FtsZ (63, 64), overexpression of FtsZ (65, 66), overexpression of the FtsZ polymerization regulator ZapA (67), and the absence of low-molecular-weight penicillin-binding proteins (LMW PBPs) (66). It is possible that the observed aberrant localization of YfiN$_{GFP}$ is due to altered polymerization of FtsZ.

Another unusual (and thus-far unique) feature of YfiN as a cell division inhibitor is that, unlike the known division inhibitors SulA (68), SidA (61), and DidA (62), cell division arrest by YfiN only leads to a modest level of cell lengthening and does not lead to filamentation (see Fig. S8 in the supplemental material). This suggests that YfiN may inhibit the synthesis of nascent PG not only at the division site but also along the lateral wall. Rod-shaped bacteria are thought to have two modes of cell wall synthesis catalyzed by different PG synthases: one responsible for cell elongation along the lateral wall and the other for the formation of the division septum (69). Our results suggest that YfiN might target a common step that these two modes share. Unlike the general inhibition of PG synthesis by β-lactam antibiotics (70, 71), the action of YfiN does not trigger cell lysis, as judged by the observation that cell density did not decrease when cell division was arrested by YfiN (Fig. 2E and 3A).

Given the positive effect of YfiN on survival under lethal PMB exposure (Fig. 7), it is tempting to speculate that the effector function of YfiN reported in this study is an adaptation mechanism that delays cell division and new peptidoglycan synthesis when E. coli cells experience envelope-disrupting environments, ensuring that the cell wall is not disarranged while the cell is recovering from the stress. Further investigation of YfiN will provide new insights into the mechanism by which bacterial cell division and cell wall synthesis are coordinated in response to environmental stress.

MATERIALS AND METHODS

Strains, growth conditions, mutagenesis, and plasmid constructions. The strains and plasmids used in this study are listed in Table S1 in the supplemental material. The wild-type parent strains for S. enterica, E. coli, and P. aeruginosa were strains 14028, MG1655, and PAO1, respectively. All strains were grown in LB broth (10 g/liter tryptone, 5 g/liter yeast extract, 5 g/liter NaCl). When appropriate, the following antibiotics were used: ampicillin (100 μg/ml), chloramphenicol (20 μg/ml), kanamycin (50 μg/ml), and gentamicin (30 μg/ml). For inducible plasmids, isopropyl-β-D-thiogalactopyranoside (IPTG) and L-arabinose were added as indicated in the figures or figure legends.

Mutants of Salmonella and E. coli were constructed by inserting a kanamycin resistance cassette into the designated gene as previously de-

scribed (72). Excision of the inserted cassettes was achieved by expression of the FLP recombinase encoded on pCP20 (72). The resulting strains were confirmed by DNA sequencing. Mutant combinations were prepared by P22 transduction.

For cloning of expression plasmids, gene sequences were amplified from the genomic DNA of wild-type strains by using PCR and introduced into pBAD30, pBAD33, pTrc99A, and pJN105. For DgcA expression vectors, pAB551, a gift from U. Jenal (40), was used as a template. Fusion proteins and an active-site mutant of YfiN were constructed using overlap extension PCR. All the resulting constructs were confirmed by DNA sequencing.

Swimming motility assay. LB swim plates were made using 0.3% Bacto agar. Plates were inoculated with 5 μl of an overnight culture in the center and incubated at 37°C for 8 h.

Fluorescence microscopy. Overnight cultures of cells with plasmids encoding fluorescent fusion proteins were diluted 1:100 in fresh LB medium with antibiotics and grown at 30°C with 0.005% arabinose for 4 h (unless otherwise stated). For imaging cells under no stress, a cell suspension (80 μl) was applied to a polylysine-coated slide, incubated for 15 min, and washed with LB medium (80 μl) before imaging. For imaging cells under stress (mostly E. coli), after 15 min of incubation, cells were washed, treated with LB containing the indicated stress-causing agent (80 μl), and incubated for 30 min before imaging. All slides for microscopy were prepared at room temperature. Stress-induced relocation was not dependent on immobilization by polylysine since it was also observed when stressors were directly added to broth cultures. For the E. coli temperature-sensitive mutants, after 30 min of stress exposure at room temperature, cells were incubated for another 30 min at the indicated temperature (30°C or 42°C) before microscopy. Images were acquired using an Olympus BX53 microscope, appropriate filters, and cellSens standard software (version 1.6) from Olympus and minimally processed using Adobe Photoshop 11.0.

HADA labeling. Nascent peptidoglycan synthesis was probed by the fluorescent D-amino acid HADA (purchased from M. van Nieuwenhze at Indiana University) as described previously (43). Salmonella enterica strain 14028 ΔyfiN bearing pBAD33 carrying ^{S}yfiN-yfp was grown at 30°C for 4 h with 0.2% glucose or 0.005% arabinose, and HADA was added to a final concentration of 500 μM. After 1 min of incubation at 30°C, cells were fixed in ice-cold 70% ethanol and incubated on ice for 15 min. The fixed cells were washed and resuspended in phosphate-buffered saline and then imaged on 1% agarose pads (43).

Bacterial two-hybrid assay. To construct plasmids used for BACTH analysis (73), gene sequences (yfiN, ftsZ, ftsA, zipA, and mreB) were amplified from the genomic DNA of wild-type E. coli MG1655 by using PCR. The amplified DNA fragments were introduced between the HindIII and XbaI sites (yfiN, ftsZ, and zipA) or the XbaI and SacI sites (ftsA) of pUT18 and pKNT25 vectors or between the XbaI and BamHI sites (mreB) of pUT18C. The E. coli K-12 strain XL1-Blue (Stratagene) was used in all of the cloning steps, and the DNA sequences of the constructs were verified by sequencing.

For interaction analysis, plasmid combinations of pUT18(C) and pKNT25 were cotransformed into the E. coli strain BTH101. Five-microliter amounts of overnight cultures of transformants were spotted onto LB agar plates supplemented with ampicillin, kanamycin, IPTG (0.5 mM), and 40 μg/ml 5-bromo-4-chloro-3-indolyl-β-D-galactopyranoside (X-Gal). For analysis of c-di-GMP-stimulated interactions, chloramphenicol and arabinose (0.2%) were additionally added to the LB agar plates. Images of the plates were taken after 36 h of incubation at 30°C.

Quantification of c-di-GMP. The c-di-GMP concentrations were measured following a previously reported method (74). E. coli MG1655 wild type and MG1655 carrying pBAD30-^{E}YfiN$_{GFP}$ were grown at 30°C for 4 h in 5 ml LB supplemented with 0.005% arabinose (the optical density at 600 nm reached around 1.2). Intracellular nucleotides were extracted with a mixture of acetonitrile-methanol-water (40:40:20, vol/vol/vol) as described previously (74). Samples were analyzed by high-

performance liquid chromatography–tandem mass spectrometry (HPLC-MS/MS) at the Metabolomics Core Facility at the University of Texas Health Science Center at San Antonio, using a Thermo Fisher Q Exactive mass spectrometer with online separation by a Thermo Fisher Dionex UltiMate 3000 HPLC instrument. As described previously (74), 0.1% (vol/vol) acetic acid in water with 10 mM ammonium acetate was used as LC solvent A, and solvent B was methanol. For a standard curve, c-di-GMP and xanthosine $3',5'$-cyclic monophosphate (cXMP) purchased from Axxora LLC (San Diego, CA) were used. As an internal standard, 1 μM cXMP was added to the extract. The result showed that the intracellular c-di-GMP concentration of cells expressing $^\mathrm{E}\mathrm{YfiN}_\mathrm{GFP}$ was 14.46 μM, while that of wild-type cells was 0.23 μM, confirming the c-di-GMP-synthetic activity of $^\mathrm{E}\mathrm{YfiN}_\mathrm{GFP}$.

SUPPLEMENTAL MATERIAL

Supplemental material for this article may be found at http://mbio.asm.org/lookup/suppl/doi:10.1128/mBio.00822-16/-/DCSupplemental.

Table S1, PDF file, 0.2 MB.
Figure S1, PDF file, 0.2 MB.
Figure S2, PDF file, 0.2 MB.
Figure S3, PDF file, 0.1 MB.
Figure S4, PDF file, 0.4 MB.
Figure S5, PDF file, 0.1 MB.
Figure S6, PDF file, 0.1 MB.
Figure S7, PDF file, 0.1 MB.
Figure S8, PDF file, 0.1 MB.

REFERENCES

1. **Hengge R.** 2009. Principles of c-di-GMP signalling in bacteria. Nat Rev Microbiol **7:**263–273. http://dx.doi.org/10.1038/nrmicro2109.
2. **Krell T, Lacal J, Busch A, Silva-Jiménez H, Guazzaroni ME, Ramos JL.** 2010. Bacterial sensor kinases: diversity in the recognition of environmental signals. Annu Rev Microbiol **64:**539–559. http://dx.doi.org/10.1146/annurev.micro.112408.134054.
3. **Wadhams GH, Armitage JP.** 2004. Making sense of it all: bacterial chemotaxis. Nat Rev Mol Cell Biol **5:**1024–1037. http://dx.doi.org/10.1038/nrm1524.
4. **Römling U, Galperin MY, Gomelsky M.** 2013. Cyclic di-GMP: the first 25 years of a universal bacterial second messenger. Microbiol Mol Biol Rev **77:**1–52. http://dx.doi.org/10.1128/MMBR.00043-12.
5. **Lori C, Ozaki S, Steiner S, Böhm R, Abel S, Dubey BN, Schirmer T, Hiller S, Jenal U.** 2015. Cyclic di-GMP acts as a cell cycle oscillator to drive chromosome replication. Nature **523:**236–239 http://dx.doi.org/10.1038/nature14473.
6. **Tamayo R, Pratt JT, Camilli A.** 2007. Roles of cyclic diguanylate in the regulation of bacterial pathogenesis. Annu Rev Microbiol **61:**131–148. http://dx.doi.org/10.1146/annurev.micro.61.080706.093426.
7. **Tuckerman JR, Gonzalez G, Gilles-Gonzalez MA.** 2011. Cyclic di-GMP activation of polynucleotide phosphorylase signal-dependent RNA processing. J Mol Biol **407:**633–639. http://dx.doi.org/10.1016/j.jmb.2011.02.019.
8. **Hoffman LR, D'Argenio DA, MacCoss MJ, Zhang Z, Jones RA, Miller SI.** 2005. Aminoglycoside antibiotics induce bacterial biofilm formation. Nature **436:**1171–1175. http://dx.doi.org/10.1038/nature03912.
9. **Tschowri N, Schumacher MA, Schlimpert S, Chinnam NB, Findlay KC, Brennan RG, Buttner MJ.** 2014. Tetrameric c-di-GMP mediates effective transcription factor dimerization to control streptomyces development. Cell **158:**1136–1147. http://dx.doi.org/10.1016/j.cell.2014.07.022.
10. **Jenal U, Malone J.** 2006. Mechanisms of cyclic-di-GMP signaling in bacteria. Annu Rev Genet **40:**385–407. http://dx.doi.org/10.1146/annurev.genet.40.110405.090423.
11. **Güvener ZT, Harwood CS.** 2007. Subcellular location characteristics of the Pseudomonas aeruginosa GGDEF protein, WspR, indicate that it produces cyclic-di-GMP in response to growth on surfaces. Mol Microbiol **66:**1459–1473. http://dx.doi.org/10.1111/j.1365-2958.2007.06008.x.
12. **Hasegawa K, Masuda S, Ono TA.** 2006. Light induced structural changes of a full-length protein and its BLUF domain in YcgF (Blrp), a blue-light sensing protein that uses FAD (BLUF). Biochemistry **45:**3785–3793. http://dx.doi.org/10.1021/bi051820x.
13. **Tuckerman JR, Gonzalez G, Sousa EH, Wan X, Saito JA, Alam M, Gilles-Gonzalez MA.** 2009. An oxygen-sensing diguanylate cyclase and phosphodiesterase couple for c-di-GMP control. Biochemistry **48:**9764–9774. http://dx.doi.org/10.1021/bi901409g.
14. **Hengge R, Galperin MY, Ghigo JM, Gomelsky M, Green J, Hughes KT, Jenal U, Landini P.** 2016. Systematic nomenclature for GGDEF and EAL domain-containing cyclic-di-GMP turnover proteins of Escherichia coli. J Bacteriol **198:**7–11 http://dx.doi.org/10.1128/JB.00424-15.
15. **Ueda A, Wood TK.** 2009. Connecting quorum sensing, c-di-GMP, pel polysaccharide, and biofilm formation in Pseudomonas aeruginosa through tyrosine phosphatase TpbA (PA3885). PLoS Pathog **5:**e1000483. http://dx.doi.org/10.1371/journal.ppat.1000483.
16. **Malone JG, Jaeger T, Spangler C, Ritz D, Spang A, Arrieumerlou C, Kaever V, Landmann R, Jenal U.** 2010. YfiBNR mediates cyclic di-GMP dependent small colony variant formation and persistence in Pseudomonas aeruginosa. PLoS Pathog **6:**e1000804. http://dx.doi.org/10.1371/journal.ppat.1000804.
17. **Le Guyon S, Simm R, Rhen M, Romling U.** 2014. Dissecting the cyclic di-GMP signaling network regulating motility in Salmonella enterica serovar Typhimurium. Environ Microbiol **17:**1310–1320. http://dx.doi.org/10.1111/1462-2920.12580.
18. **Hufnagel DA, DePas WH, Chapman MR.** 2014. The disulfide bonding system suppresses CsgD-independent cellulose production in Escherichia coli. J Bacteriol **196:**3690–3699. http://dx.doi.org/10.1128/JB.02019-14.
19. **Malone JG, Jaeger T, Manfredi P, Dötsch A, Blanka A, Bos R, Cornelis GR, Häussler S, Jenal U.** 2012. The YfiBNR signal transduction mechanism reveals novel targets for the evolution of persistent Pseudomonas aeruginosa in cystic fibrosis airways. PLoS Pathog **8:**e1002760. http://dx.doi.org/10.1371/journal.ppat.1002760.
20. **Raterman EL, Shapiro DD, Stevens DJ, Schwartz KJ, Welch RA.** 2013. Genetic analysis of the role of yfiR in the ability of Escherichia coli CFT073 to control cellular cyclic dimeric GMP levels and to persist in the urinary tract. Infect Immun **81:**3089–3098. http://dx.doi.org/10.1128/IAI.01396-12.
21. **Adams DW, Errington J.** 2009. Bacterial cell division: assembly, maintenance and disassembly of the Z ring. Nat Rev Microbiol **7:**642–653. http://dx.doi.org/10.1038/nrmicro2198.
22. **Margolin W.** 2005. FtsZ and the division of prokaryotic cells and organelles. Nat Rev Mol Cell Biol **6:**862–871. http://dx.doi.org/10.1038/nrm1745.
23. **Egan AJ, Vollmer W.** 2013. The physiology of bacterial cell division. Ann N Y Acad Sci **1277:**8–28. http://dx.doi.org/10.1111/j.1749-6632.2012.06818.x.
24. **Aarsman ME, Piette A, Fraipont C, Vinkenvleugel TM, Nguyen-Distèche M, den Blaauwen T.** 2005. Maturation of the Escherichia coli divisome occurs in two steps. Mol Microbiol **55:**1631–1645. http://dx.doi.org/10.1111/j.1365-2958.2005.04502.x.
25. **Pichoff S, Lutkenhaus J.** 2002. Unique and overlapping roles for ZipA and FtsA in septal ring assembly in Escherichia coli. EMBO J **21:**685–693. http://dx.doi.org/10.1093/emboj/21.4.685.
26. **Jonas K.** 2014. To divide or not to divide: control of the bacterial cell cycle by environmental cues. Curr Opin Microbiol **18:**54–60. http://dx.doi.org/10.1016/j.mib.2014.02.006.
27. **Weart RB, Lee AH, Chien AC, Haeusser DP, Hill NS, Levin PA.** 2007. A metabolic sensor governing cell size in bacteria. Cell **130:**335–347. http://dx.doi.org/10.1016/j.cell.2007.05.043.
28. **Huisman O, D'Ari R.** 1981. An inducible DNA replication-cell division coupling mechanism in E. coli. Nature **290:**797–799. http://dx.doi.org/10.1038/290797a0.
29. **Miller C, Thomsen LE, Gaggero C, Mosseri R, Ingmer H, Cohen SN.** 2004. SOS response induction by beta-lactams and bacterial defense against antibiotic lethality. Science **305:**1629–1631. http://dx.doi.org/10.1126/science.1101630.

30. **Paul K, Nieto V, Carlquist WC, Blair DF, Harshey RM**. 2010. The c-di-GMP binding protein YcgR controls flagellar motor direction and speed to affect chemotaxis by a "backstop brake" mechanism. Mol Cell **38**:128–139. http://dx.doi.org/10.1016/j.molcel.2010.03.001.

31. **Boehm A, Kaiser M, Li H, Spangler C, Kasper CA, Ackermann M, Kaever V, Sourjik V, Roth V, Jenal U**. 2010. Second messenger-mediated adjustment of bacterial swimming velocity. Cell **141**:107–116. http://dx.doi.org/10.1016/j.cell.2010.01.018.

32. **Abel S, Chien P, Wassmann P, Schirmer T, Kaever V, Laub MT, Baker TA, Jenal U**. 2011. Regulatory cohesion of cell cycle and cell differentiation through interlinked phosphorylation and second messenger networks. Mol Cell **43**:550–560. http://dx.doi.org/10.1016/j.molcel.2011.07.018.

33. **Lindenberg S, Klauck G, Pesavento C, Klauck E, Hengge R**. 2013. The EAL domain protein YciR acts as a trigger enzyme in a c-di-GMP signalling cascade in E. coli biofilm control. EMBO J **32**:2001–2014. http://dx.doi.org/10.1038/emboj.2013.120.

34. **Dahlstrom KM, Giglio KM, Collins AJ, Sondermann H, O'Toole GA**. 2015. Contribution of physical interactions to signaling specificity between a diguanylate cyclase and its effector. mBio **6**:e01978-15. http://dx.doi.org/10.1128/mBio.01978-15.

35. **Ben-Yehuda S, Losick R**. 2002. Asymmetric cell division in B. subtilis involves a spiral-like intermediate of the cytokinetic protein FtsZ. Cell **109**:257–266. http://dx.doi.org/10.1016/S0092-8674(02)00698-0.

36. **Thanedar S, Margolin W**. 2004. FtsZ exhibits rapid movement and oscillation waves in helix-like patterns in Escherichia coli. Curr Biol **14**:1167–1173. http://dx.doi.org/10.1016/j.cub.2004.06.048.

37. **Specht M, Dempwolff F, Schätzle S, Thomann R, Waidner B**. 2013. Localization of FtsZ in Helicobacter pylori and consequences for cell division. J Bacteriol **195**:1411–1420. http://dx.doi.org/10.1128/JB.01490-12.

38. **Shih YL, Kawagishi I, Rothfield L**. 2005. The MreB and Min cytoskeletal-like systems play independent roles in prokaryotic polar differentiation. Mol Microbiol **58**:917–928. http://dx.doi.org/10.1111/j.1365-2958.2005.04841.x.

39. **Mukherjee A, Cao C, Lutkenhaus J**. 1998. Inhibition of FtsZ polymerization by SulA, an inhibitor of septation in Escherichia coli. Proc Natl Acad Sci U S A **95**:2885–2890. http://dx.doi.org/10.1073/pnas.95.6.2885.

40. **Steiner S, Lori C, Boehm A, Jenal U**. 2013. Allosteric activation of exopolysaccharide synthesis through cyclic di-GMP-stimulated protein-protein interaction. EMBO J **32**:354–368. http://dx.doi.org/10.1038/emboj.2012.315.

41. **Busiek KK, Margolin W**. 2014. A role for FtsA in SPOR-independent localization of the essential Escherichia coli cell division protein FtsN. Mol Microbiol **92**:1212–1226. http://dx.doi.org/10.1111/mmi.12623.

42. **Pichoff S, Du S, Lutkenhaus J**. 2015. The bypass of ZipA by overexpression of FtsN requires a previously unknown conserved FtsN motif essential for FtsA-FtsN interaction supporting a model in which FtsA monomers recruit late cell division proteins to the Z ring. Mol Microbiol **95**:971–987. http://dx.doi.org/10.1111/mmi.12907.

43. **Kuru E, Tekkam S, Hall E, Brun YV, Van Nieuwenhze MS**. 2015. Synthesis of fluorescent D-amino acids and their use for probing peptidoglycan synthesis and bacterial growth in situ. Nat Protoc **10**:33–52. http://dx.doi.org/10.1038/nprot.2014.197.

44. **Vaara M**. 1992. Agents that increase the permeability of the outer membrane. Microbiol Rev **56**:395–411.

45. **Daugelavicius R, Bakiene E, Bamford DH**. 2000. Stages of polymyxin B interaction with the Escherichia coli cell envelope. Antimicrob Agents Chemother **44**:2969–2978. http://dx.doi.org/10.1128/AAC.44.11.2969-2978.2000.

46. **Hancock REW**. 1984. Alterations in outer membrane permeability. Annu Rev Microbiol **38**:237–264. http://dx.doi.org/10.1146/annurev.mi.38.100184.001321.

47. **Cascales E, Bernadac A, Gavioli M, Lazzaroni JC, Lloubes R**. 2002. Pal lipoprotein of Escherichia coli plays a major role in outer membrane integrity. J Bacteriol **184**:754–759. http://dx.doi.org/10.1128/JB.184.3.754-759.2002.

48. **Gerding MA, Ogata Y, Pecora ND, Niki H, de Boer PA**. 2007. The trans-envelope Tol-Pal complex is part of the cell division machinery and required for proper outer-membrane invagination during cell constriction in E. coli. Mol Microbiol **63**:1008–1025. http://dx.doi.org/10.1111/j.1365-2958.2006.05571.x.

49. **Addinall SG, Bi E, Lutkenhaus J**. 1996. FtsZ ring formation in fts mutants. J Bacteriol **178**:3877–3884.

50. **Varma A, Young KD**. 2004. FtsZ collaborates with penicillin binding proteins to generate bacterial cell shape in Escherichia coli. J Bacteriol **186**:6768–6774. http://dx.doi.org/10.1128/JB.186.20.6768-6774.2004.

51. **Karimova G, Dautin N, Ladant D**. 2005. Interaction network among Escherichia coli membrane proteins involved in cell division as revealed by bacterial two-hybrid analysis. J Bacteriol **187**:2233–2243. http://dx.doi.org/10.1128/JB.187.7.2233-2243.2005.

52. **Fenton AK, Gerdes K**. 2013. Direct interaction of FtsZ and MreB is required for septum synthesis and cell division in Escherichia coli. EMBO J **32**:1953–1965. http://dx.doi.org/10.1038/emboj.2013.129.

53. **Schirmer T, Jenal U**. 2009. Structural and mechanistic determinants of c-di-GMP signalling. Nat Rev Microbiol **7**:724–735. http://dx.doi.org/10.1038/nrmicro2203.

54. **Yang X, Yang XA, Xu M, Zhou L, Fan Z, Jiang T**. 2015. Crystal structures of YfiR from Pseudomonas aeruginosa in two redox states. Biochem Biophys Res Commun **461**:14–20 http://dx.doi.org/10.1016/j.bbrc.2015.03.160.

55. **Ross P, Weinhouse H, Aloni Y, Michaeli D, Weinberger-Ohana P, Mayer R, Braun S, de Vroom E, van der Marel GA, van Boom JH, Benziman M**. 1987. Regulation of cellulose synthesis in Acetobacter xylinum by cyclic diguanylic acid. Nature **325**:279–281. http://dx.doi.org/10.1038/325279a0.

56. **Dixon RA, Chopra I**. 1986. Leakage of periplasmic proteins from Escherichia coli mediated by polymyxin B nonapeptide. Antimicrob Agents Chemother **29**:781–788. http://dx.doi.org/10.1128/AAC.29.5.781.

57. **Anraku Y, Heppel LA**. 1967. On the nature of the changes induced in Escherichia coli by osmotic shock. J Biol Chem **242**:2561–2569.

58. **Chou SH, Galperin MY**. 2016. Diversity of cyclic di-GMP-binding proteins and mechanisms. J Bacteriol **198**:32–46. http://dx.doi.org/10.1128/JB.00333-15.

59. **Yang CY, Chin KH, Chuah ML, Liang ZX, Wang AH, Chou SH**. 2011. The structure and inhibition of a GGDEF diguanylate cyclase complexed with (c-di-GMP)(2) at the active site. Acta Crystallogr D Biol Crystallogr **67**:997–1008. http://dx.doi.org/10.1107/S090744491104039X.

60. **Reinders A, Hee CS, Ozaki S, Mazur A, Boehm A, Schirmer T, Jenal U**. 2016. Expression and genetic activation of cyclic di-GMP-specific phosphodiesterases in Escherichia coli. J Bacteriol **198**:448–462. http://dx.doi.org/10.1128/JB.00604-15.

61. **Modell JW, Hopkins AC, Laub MT**. 2011. A DNA damage checkpoint in Caulobacter crescentus inhibits cell division through a direct interaction with FtsW. Genes Dev **25**:1328–1343. http://dx.doi.org/10.1101/gad.2038911.

62. **Modell JW, Kambara TK, Perchuk BS, Laub MT**. 2014. A DNA damage-induced, SOS-independent checkpoint regulates cell division in Caulobacter crescentus. PLoS Biol **12**:e1001977. http://dx.doi.org/10.1371/journal.pbio.1001977.

63. **Addinall SG, Lutkenhaus J**. 1996. FtsZ-spirals and -arcs determine the shape of the invaginating septa in some mutants of Escherichia coli. Mol Microbiol **22**:231–237. http://dx.doi.org/10.1046/j.1365-2958.1996.00100.x.

64. **Stricker J, Erickson HP**. 2003. In vivo characterization of Escherichia coli ftsZ mutants: effects on Z-ring structure and function. J Bacteriol **185**:4796–4805. http://dx.doi.org/10.1128/JB.185.16.4796-4805.2003.

65. **Ma X, Ehrhardt DW, Margolin W**. 1996. Colocalization of cell division proteins FtsZ and FtsA to cytoskeletal structures in living Escherichia coli cells by using green fluorescent protein. Proc Natl Acad Sci U S A **93**:12998–13003. http://dx.doi.org/10.1073/pnas.93.23.12998.

66. **Potluri LP, de Pedro MA, Young KD**. 2012. Escherichia coli low-molecular-weight penicillin-binding proteins help spatial septal FtsZ, and their absence leads to asymmetric cell division and branching. Mol Microbiol **84**:203–224. http://dx.doi.org/10.1111/j.1365-2958.2012.08023.x.

67. **Galli E, Gerdes K**. 2012. FtsZ-ZapA-ZapB interactome of Escherichia coli. J Bacteriol **194**:292–302. http://dx.doi.org/10.1128/JB.05821-11.

68. **Huisman O, D'Ari R, Gottesman S**. 1984. Cell-division control in Escherichia coli: specific induction of the SOS function SfiA protein is sufficient to block septation. Proc Natl Acad Sci U S A **81**:4490–4494. http://dx.doi.org/10.1073/pnas.81.14.4490.

69. **Scheffers DJ, Pinho MG**. 2005. Bacterial cell wall synthesis: new insights from localization studies. Microbiol Mol Biol Rev **69**:585–607. http://dx.doi.org/10.1128/MMBR.69.4.585-607.2005.

70. **Chung HS, Yao Z, Goehring NW, Kishony R, Beckwith J, Kahne D**. 2009. Rapid beta-lactam-induced lysis requires successful assembly of the

cell division machinery. Proc Natl Acad Sci U S A **106:**21872–21877. http://dx.doi.org/10.1073/pnas.0911674106.

71. **Tomasz A**. 1979. The mechanism of the irreversible antimicrobial effects of penicillins: how the beta-lactam antibiotics kill and lyse bacteria. Annu Rev Microbiol **33:**113–137. http://dx.doi.org/10.1146/annurev.mi.33.100179.000553.

72. **Datsenko KA, Wanner BL**. 2000. One-step inactivation of chromosomal genes in Escherichia coli K-12 using PCR products. Proc Natl Acad Sci U S A **97:**6640–6645. http://dx.doi.org/10.1073/pnas.120163297.

73. **Karimova G, Pidoux J, Ullmann A, Ladant D**. 1998. A bacterial two-hybrid system based on a reconstituted signal transduction pathway. Proc Natl Acad Sci U S A **95:**5752–5756. http://dx.doi.org/10.1073/pnas.95.10.5752.

74. **Spangler C, Böhm A, Jenal U, Seifert R, Kaever V**. 2010. A liquid chromatography-coupled tandem mass spectrometry method for quantitation of cyclic di-guanosine monophosphate. J Microbiol Methods **81:**226–231. http://dx.doi.org/10.1016/j.mimet.2010.03.020.

75. **Fang X, Gomelsky M**. 2010. A post-translational, c-di-GMP-dependent mechanism regulating flagellar motility. Mol Microbiol **76:**1295–1305.